

NICMOS and VLBA observations of the gravitational lens system B1933+503

D. R. Marlow, I. W. A. Browne, N. Jackson & P. N. Wilkinson

University of Manchester, NRAL Jodrell Bank, Macclesfield, Cheshire SK11 9DL, England

August 20, 1998

ABSTRACT

NICMOS observations of the complex gravitational lens system B1933+503 reveal infrared counterparts to two of the inverted spectrum radio images. The infrared images have arc-like structures. The corresponding radio images are also detected in a VLBA map made at 1.7-GHz with a resolution of 6 mas. We fail to detect two of the four inverted radio spectrum components with the VLBA even though they are clearly visible in a MERLIN map at the same frequency at a different epoch. The absence of these two components could be due to rapid variability on a time-scale less than the time delay, or to broadening of the images during propagation of the radio waves through the ISM of the lensing galaxy to an extent that they fall below the surface brightness detectability threshold of the VLBA observations. The failure to detect the same two images with NICMOS is probably due to extinction in the ISM of the lensing galaxy.

Key words: gravitational lensing; individual systems; B1933+503 – galaxies; structure

1 INTRODUCTION

The Cosmic Lens All-Sky Survey (CLASS) is a survey of flat-spectrum radio sources whose primary purpose is the discovery of new radio-loud gravitational lens systems (Browne et al. 1997; Myers et al. 1999). A survey of $\sim 15,000$ radio sources has been made. The discovery of the complex lens system B1933+503 has been reported by Sykes et al. (1998) and a discussion of the lens model has been given in Nair (1998). The radio maps (see Figure 1) show nine components, one of which (labelled 2) probably consists of two blended images. The lens model indicates that the unlensed radio source has an almost linear, three-component structure on a scale of 200–250 mas, with an inverted-spectrum component in the middle. Two of its components are quadruply imaged and the third is doubly imaged. Evidence for flux density variability at a wavelength of 2 cm is reported by Sykes et al. (1998). The images corresponding to the central component of the source are compact in MERLIN maps (labelled 1, 3, 4 and 6). Sykes et al. (1998) compare MERLIN and VLA maps and find that the images of the central component have inverted radio spectra. The relative flux densities of these inverted spectrum components appear to have varied. The other images have steep spectra and some are extended on the scale of ~ 100 mas.

Sykes et al. (1998) also show an HST WFPC2 picture of the B1933+503 system taken through an I-band filter (F814W). The lensing galaxy is clearly seen but no coun-

terparts to any of the lensed images are detected down to a limit of about magnitude 24.2 in I. A redshift of 0.755 has been measured for the lensing galaxy (Sykes et al. 1998).

The presence of many images means that the lens mass model is well constrained and the fact that some of the images are variable means that it should be possible to measure time delays and hence determine the Hubble constant. Because this is such a promising system we have embarked on a systematic programme to obtain observational constraints for the mass model. In this paper we present HST NICMOS H-band observations that reveal for the first time infrared counterparts to two of the radio images. We also present a high resolution VLBA 1.7-GHz map which shows even more complex radio structure than has been seen before. We discuss reasons why the flux density ratios of the images are very different when measured with NICMOS and the VLBA to those measured with MERLIN and the VLA.

2 NICMOS OBSERVATIONS

NICMOS observations of B1933+503 were made on October 9, 1997. The NIC1 camera was used providing a pixel scale of 43 mas/pixel. A fit to the point spread function generated by the TinyTim program (Krist 1997) yields a FWHM of 131 mas for the NICMOS observations. The F160W spectral filter was used which has a central wavelength of $1.6\mu\text{m}$ and

arXiv:astro-ph/9810452v1 28 Oct 1998

corresponds roughly to H-band. The total integration time was 10495 seconds.

Both the lensing galaxy and two extended arc-like features (hereinafter arcs) were detected. Parameters measured from the NICMOS picture are listed in Table 1. The arcs correspond exactly in separation and position angle to images 1 and 4 seen in the radio maps (see Figure 1). Moreover, the best-fit lens model described by Nair (1998) yields a lens centre (with respect to component 4) at (RA, Dec) 423_{-5}^{+9} , 270_{-5}^{+7} mas – within ~ 15 mas of the observed NICMOS separation of $417, 282 \pm 10$ mas.

Thus there is no doubt that the arcs are gravitational lens images of the host of the compact radio source. The fact that arcs rather than point sources are detected indicates that extended starlight dominates any emission from a compact active nucleus in the lensed object. Remarkably, no infrared emission is detected from the positions of the other compact, inverted spectrum, radio components 3 and 6, indicating that the ratios of their flux densities with component 1 must be < 0.1 . In the VLA and MERLIN radio maps presented by Sykes et al. (see their Table 2) the 3 to 1 and 6 to 1 ratios are typically ~ 0.7 ; i.e. very different from those in the infrared. We discuss this discrepancy and a similar one in the VLBA ratios in Section 4.

3 VLBA 1.7-GHZ OBSERVATIONS

The VLBA 1.7-GHz observations were made on June 25, 1996. Phase referencing was performed by alternately observing the strong calibrator source B1954+51 and the target source over the total integration time of 15 hours. One VLA antenna was included in the array to improve coverage of the uv plane over short spacings and to increase sensitivity to weak and extended structure. Fringe fitting was performed using B1954+51 and the residual phase errors were corrected over the whole data set. The data reduction was performed in AIPS and mapping was performed using DIFMAP, part of the Caltech VLBI package (Shepherd et al. 1994).

The naturally-weighted full-resolution VLBA map is shown in Figure 1. The resolution of the map is 6 mas and it has a noise level of $38 \mu\text{Jy}$. A separate map convolved with a 20 mas FWHM beam is also shown. Individual component flux densities measured from the different maps are listed in Table 1.

There are several noteworthy results of these observations: The images 2 and 5 are highly stretched into arc-like features consistent with the MERLIN map; images of the inverted spectrum components 1 and 4 are clearly detected and component 4 has been resolved; there is no sign of the other inverted spectrum components 3 and 6 even though they are clearly present in the MERLIN L-band map (Figure 1).

The $5\text{-}\sigma$ detection limit on components 3 and 6 is roughly an order of magnitude less than the 2.5 mJy and 2.2 mJy seen in the MERLIN map. In order to search for some evidence of the missing images a map was constructed from the VLBA data using only the shortest (0–5M λ) baselines. In this map there were $2\text{-}\sigma$ hints of components 3 and 6 at the sub-mJy level suggesting perhaps that they are highly resolved and have structure on the scale of ~ 50 mas.

4 DISCUSSION

The B1933+503 system is in many ways a promising one to use for the determination of the Hubble constant from time delays because of its reported variability and the multiple constraints on the mass model. However, the lack of a redshift for, or even the detection of, the lensed object has hitherto been a problem. The detection with NICMOS of infrared emission from the lensed object now gives hope that a redshift can be obtained. The fact that the NICMOS picture shows extended arcs of emission rather than point sources suggests that we are detecting the lensed emission from an intrinsically extended source. This is consistent with the faintness of the two images. Assuming no extinction, if the lensed object has the luminosity of an elliptical L^* galaxy, we would expect it to have approximately the observed magnitude of $H=22.1$ for $z \lesssim 2$ (Poggianti 1997). Since lensing also magnifies the images by about a magnitude the faintness of the objects implies one or more of the following: the lensed object is sub- L^* , it is $z \gtrsim 2$, or it suffers extinction in the lensing galaxy.

The failure to detect images 3 and 6 in the NICMOS picture and in the 1.7-GHz VLBA maps (Figure 1) is intriguing. For the radio case we consider two possibilities; either a combination of rapid variability and lens time delay have conspired to move the images below the detection limit of our VLBA observations, or they are of much lower surface brightness (e.g. due to scattering) than the other images and have been resolved out. We find neither explanation compelling. The latter seems unlikely, firstly because components 3 and 6 were detected in September 1995 in 1 mas resolution, VLBA 5-GHz snapshot observations (Sykes et al. 1998), (this result was consistent with the expectation that inverted spectrum radio components should be compact), and secondly, because the weaker, lower magnification, images should be more compact than the stronger images. However, it is possible that the images could be scattered broadened by passage through the ISM of the lensing galaxy. This is supported by the hint of a detection of these images in the highly tapered VLBA 1.7-GHz map, suggesting that they may have a much larger angular size than the corresponding images 1 and 4. In another lens system, 0218+357, there is a strong dependence of the image size on frequency of observation (Patnaik and Porcas 1998) and it is quite likely that this arises from interstellar scattering in the ISM of the lensing galaxy (Wilkinson et al. 1998).

We must also consider the variability explanation for the non-detection of images 3 and 6 in the VLBA map. There is already evidence of relative variability amongst images 1, 3, 4 and 6 from VLA 2-cm observations (Sykes et al. 1998) of a few tens of percent. However, in extragalactic radio sources, flux density variations at wavelengths around 18 cm are usually less than a few tens of percent and occur on time-scales of months (Webber et al. 1980). This lack of variability is also well illustrated by a comparison of the flux densities of sources in the 1.4-GHz NVSS (Condon et al. 1998) and FIRST (Becker et al. 1995) catalogues. The observations for the catalogues were taken at least six months apart, but $\ll 1\%$ of sources have flux densities that differ by $> 30\%$. In order for the explanation to work in B1933+503 the variability must occur on a timescale shorter than the time delays. Since the redshift of the lensed object is

unknown the predicted time delays have some uncertainty. However, Nair (1998) suggests the delays with respect to component 1 should be approximately 8 days for component 3, 7 days for component 4 and 9 days for component 6. Thus the timescale of the variability must be shorter than a few days. The required amplitude of the variability can be estimated from comparing the flux densities in the MERLIN 18cm map (Figure 1) with the detection limit on the present VLBA map. Components 3 and 6 need to have decreased in flux density by nearly an order of magnitude in a couple of days. We conclude that the explanation, though theoretically possible, requires such extreme variability properties for B1933+503 as to render it highly unlikely.

It is perhaps significant that the same two images (3 and 6) are also not detected in the NICMOS image. If variability were the explanation for both the radio and infrared non-detections, we would have to attribute the fact that the same two images are missing to coincidence since radio and optical variability are hardly ever correlated and, moreover, the NICMOS and VLBA observations are separated in time by far longer than the expected time delays. Rapid variability of the infrared emission also seems physically implausible given that the images are extended and are therefore dominated by starlight. It is, therefore, much more likely that in the infrared images 3 and 6 are weaker relative to 1 and 4 than they are in the low resolution radio maps due to infrared extinction. Supporting this view is the fact that both 3 and 6 lie along the major axis of the lensing galaxy where one might *a priori* expect there to be higher extinction. The amount of extinction required is large enough ($A_V \sim 10$) to suggest that there might also be ionized gas present along the line of sight, maybe enough to give rise to sufficient multi-path scattering to cause the images to be resolved with the VLBA. We note that in B0218+357, the other lensed system for which there is evidence of scatter broadening of the radio components, there is also evidence for large extinction occurring in the lensing galaxy (Xanthopoulos et al. 1998). In the case of B0218+357 it is known that the lens is a spiral galaxy. Perhaps this is also the case for B1933+503.

5 CONCLUSIONS

The presence of copious extended structure in our VLBA map means that even more observational constraints are now available for the lens mass model.

With the current data it is premature to reach a firm conclusion about why the VLBA and infrared image flux ratios are so different from the MERLIN and VLA ratios reported by Sykes et al. (1998). It seems very plausible that extinction is responsible for the dimming of the images in the NICMOS image. We also favour the multi-path scattering explanation for the non-detection of the corresponding radio images. Clearly a radio map with better surface brightness sensitivity should tell us the answer and we are planning to make global VLBI observations for this purpose. On the other hand, if it turns out that variability is the answer, then B1933+503 is indeed an exciting object for time delay measurement and Hubble constant determination. VLA monitoring observations are in progress.

ACKNOWLEDGMENTS

This research used observations with the Hubble Space Telescope, obtained at the Space Telescope Science Institute, which is operated by Associated Universities for Research in Astronomy Inc. under NASA contract NAS5-26555. The VLBA is operated by Associated Universities for Research in Astronomy Inc. on behalf of the National Science Foundation. MERLIN is operated as a National Facility by NRAL, University of Manchester, on behalf of the UK Particle Physics & Astronomy Research Council. This work is supported in part by the European Commission, TMR Programme, Research Network Contract ERBFMRXCT96-0034 "CERES". DRM is supported by a PPARC studentship. We are grateful to P. Helbig and L. Koopmans for their assistance with this work.

REFERENCES

- Becker, R.H., White, R.L. & Helfand, D.J. 1995, ApJ, 450, 559
 Browne, I.W.A., Jackson, N.J., Augusto, P., Henstock, D.R. Marlow, D.R., Nair, S. & Wilkinson, P.N., 1997, *Cosmology with the new radio surveys*, eds Bremer, M., Jackson, N.J, I. Pérez-Fournon (Kluwer Academic Publishers)
 Condon, J.J., Cotton, W.D., Greisen, E.W., Yin, Q.F., Perley, R.A., Taylor, G.B., & Broderick, J.J. 1998, AJ, 115, 1693
 Krist, J., 1997, "The TinyTim user guide", available at <http://scivax.stsci.edu/~krist/tinytim.html>
 Myers, S., et al., 1999, in preparation
 Nair, S. 1998, MNRAS, submitted, astro-ph/9803076.
 Patnaik, A.R., Porcas, R.W. 1998, Highly redshifted radio lines, eds C. Carilli, S. Radford, K. Menten, G. Langston (PASP Conference series)
 Pogianti, B.M., 1997, A&AS, 122, 399
 Shepherd, M.C., Pearson, T.J. & Taylor, G.B. 1994, BASS, 26, 987
 Sykes, C.M. et al., 1998, MNRAS, submitted, astro-ph/9710358
 Webber, J.C., Yang, J.S., Swenson, G.W. 1980, AJ, 85, 1434
 Wilkinson, P.N. et al., 1998, in preparation
 Xanthopoulos, A. et al., 1998, MNRAS, submitted

Figure 1. MERLIN, VLBA and NICMOS images of B1933+503. Top left: MERLIN 1.7-GHz map convolved with a 100 mas beam. Contours are plotted at $-2.5, 2.5, 5, 10, 20, 40, 80\%$ of the peak flux density of 16.6 mJy/beam . The individual components are numbered 1a-8. The map is centred on RA 19 34 30.950 Dec $+50 25 23.600$ (J2000). Top right: VLBA 1.7-GHz map naturally-weighted map at full-resolution. Contours are plotted at $-1.5, 1.5, 3, 6, 12, 24, 48, 96\%$ of the peak flux density of 11.5 mJy/beam . The noise level in the map is $38 \mu\text{Jy}$. The map is centred on RA 19 34 30.932 Dec $+50 25 23.502$ (J2000). Bottom left: The VLBA 1.7-GHz map convolved with a 20 mas beam. Contours are plotted at $-1.5, 1.5, 3, 6, 12, 24, 48, 96\%$ of the peak flux density of 13.1 mJy/beam . The noise level in the map is $45 \mu\text{Jy}$. Bottom right: NICMOS $1.6 \mu\text{m}$ image showing the lensing galaxy and two of the lensed components. The expected positions of the other lensed images relative to components 1 and 4 (as measured from the MERLIN 1.7-GHz map) are overlaid on to the NICMOS figure.

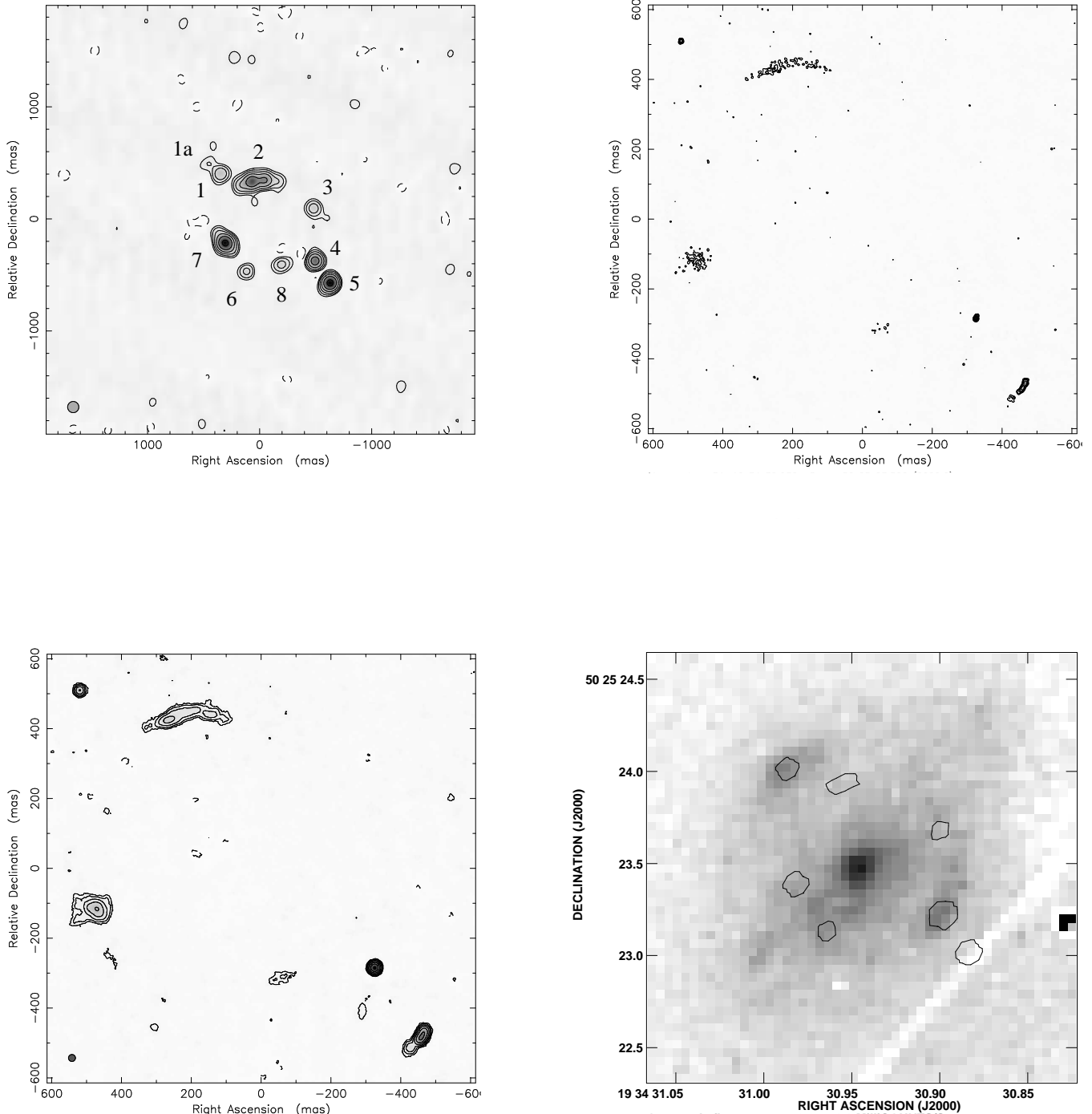


Table 1. Radio and F160W image flux densities and positions. Flux densities of components in the NICMOS image at $1.6\mu\text{m}$ are given in the second column. The total integration time was 10495 seconds. Radio flux densities in various maps are quoted in columns 3, 4 and 5. Typical flux density errors are ± 0.4 mJy. Values for the MERLIN observations of October 27, 1995 are taken from Sykes et al. (1998). Values are quoted for the VLBA observation in maps at the natural resolution of 6 mas and in one convolved with a 20 mas beam. Detection limits at 5σ are quoted for the missing components. Positions are given (in mas) for the the two lensed images 1 and 4 measured from the NICMOS image relative to the lensing galaxy centre.

Cmpt.	Flux density $1.6\mu\text{m}$ ($\times 10^{-20} \text{Wm}^{-2} \text{nm}^{-1}$)	Flux density MERLIN 1.7-GHz mJy/b (100 mas)	Flux density VLBA 1.7-GHz mJy/b (20 mas)	Flux density VLBA 1.7-GHz mJy/b (6 mas)	Offset from galaxy centre NICMOS (RA,Dec,error)
1a	< 0.02	0.9	< 0.22	< 0.19	-
1	0.177 ± 0.01	3.6	3.5	3.7	$406,538 \pm 10$
2	< 0.02	23.0	19.3	35.9	-
3	< 0.02	2.5	< 0.22	< 0.19	-
4	0.180 ± 0.01	9.4	13.7	14.2	$-417, -282 \pm 10$
5	< 0.02	16.2	18.3	18.7	-
6	< 0.02	2.2	< 0.22	< 0.19	-
7	< 0.02	20.3	18.2	20.4	-
8	< 0.02	3.6	1.7	3.6	-
Gal	5.400 ± 0.30	-	-	-	0,0